

UCSF

UC San Francisco Previously Published Works

Title

Selective isoxazolopyrimidine PAT1 (SLC26A6) inhibitors for therapy of intestinal disorders.

Permalink

<https://escholarship.org/uc/item/6fk419hr>

Journal

MedChemComm, 14(11)

Authors

Chu, Tiffany
Karmakar, Joy
Haggie, Peter
[et al.](#)

Publication Date

2023-11-15

DOI

10.1039/d3md00302g


Peer reviewed

RESEARCH ARTICLE



Cite this: *RSC Med. Chem.*, 2023, 14, 2342

Selective isoxazolopyrimidine PAT1 (SLC26A6) inhibitors for therapy of intestinal disorders†

Tifany Chu,^a Joy Karmakar,^a Peter M. Haggie,^b Joseph-Anthony Tan,^b Riya Master,^a Keerthana Ramaswamy,^a Alan S. Verkman,^b Marc O. Anderson^c and Onur Cil ^{*a}

A loss of prosecretory Cl⁻ channel CFTR activity in the intestine is considered as the key cause of gastrointestinal problems in cystic fibrosis (CF): meconium ileus, distal intestinal obstruction syndrome (DIOS) and constipation. Since CFTR modulators have minimal effects on gastrointestinal symptoms, there is an unmet need for novel treatments for CF-associated gastrointestinal disorders. Meconium ileus and DIOS mainly affect the ileum (distal small intestine). SLC26A6 (putative anion transporter 1, PAT1) is a Cl⁻/HCO₃⁻ exchanger at the luminal membrane of small intestinal epithelial cells which facilitates Cl⁻ and fluid absorption. We recently identified first-in-class PAT1 inhibitors by high-throughput screening. Isoxazolopyrimidine PAT1_{inh}-A01 was a hit compound, which had low potency (IC₅₀ 5.2 μM) for SLC26A6 inhibition precluding further preclinical development. Here we performed structure–activity relationship studies to optimize isoxazolopyrimidine SLC26A6 inhibitors and tested a potent inhibitor in mouse models of intestinal fluid absorption. Structure–activity studies of 377 isoxazolopyrimidine analogs identified PAT1_{inh}-A0030 (ethyl 4-(benzyl(methyl)amino)-3-methylisoxazolo[5,4-d]pyrimidine-6-carboxylate) as the most potent SLC26A6 inhibitor with a 1.0 μM IC₅₀. Selectivity studies showed that PAT1_{inh}-A030 has no activity on relevant ion transporters/channels (SLC26A3, SLC26A4, SLC26A9, CFTR, TMEM16A). In a closed-loop model of intestinal fluid absorption, intraluminal PAT1_{inh}-A0030 treatment inhibited fluid absorption in the ileum of wild-type and CF mice (*Cfr*^{delF508/delF508}) with >90% prevention of a decrease in loop fluid volume and loop weight/length ratio at 30 minutes. These results suggest that SLC26A6 is the key transporter mediating Cl⁻ and fluid absorption in the ileum and SLC26A6 inhibitors are novel drug candidates for treatment of CF-associated small intestinal disorders.

Received 30th June 2023,
Accepted 10th September 2023

DOI: 10.1039/d3md00302g

rsc.li/medchem

Introduction

Meconium ileus, distal intestinal obstruction syndrome (DIOS) and constipation are common gastrointestinal (GI) problems in cystic fibrosis (CF).¹ A loss of prosecretory Cl⁻ channel CFTR function in the intestine is considered as the key cause of these GI disorders, which are characterized by dehydration of the luminal contents.² Meconium ileus and DIOS primarily affect the distal small intestine (ileum), whereas constipation is mainly a colonic problem. Although CFTR modulators are highly effective in lung diseases in CF, they have minimal effects on GI symptoms.³ Thus, there is an unmet clinical need for novel treatments for CF-associated GI disorders.

Solute carrier (SLC) transporters are a family of several membrane proteins that transport ions and other solutes across biological membranes.⁴ SLC26 family transporters are a subgroup of SLCs which are expressed in many tissues including the intestine, kidneys and lungs, and mediate the transport of anions (Cl⁻, HCO₃⁻, oxalate, sulfate, *etc.*) across the plasma membrane.⁵ Thus, SLC26 anion exchangers are novel drug targets for gastrointestinal, kidney and pulmonary diseases.^{6–11} In intestinal epithelia, SLC26A3 (down-regulated in adenoma, DRA) and SLC26A6 (putative anion transporter 1, PAT1) are the major Cl⁻/HCO₃⁻ exchangers expressed in the luminal plasma membrane where they facilitate Cl⁻ and fluid absorption.¹² DRA is primarily expressed in the colon, whereas PAT1 is expressed in the small intestine.^{13,14} Since meconium ileus and DIOS mainly affect the ileum, the distal portion of the small intestine, by blocking Cl⁻ and fluid absorption, PAT1 inhibition can hydrate the luminal contents independent of CFTR for treatment of CF-associated small intestinal disorders. We recently identified first-in-class PAT1 inhibitors by high-throughput screening of 50 000 compounds in Fischer rat thyroid (FRT) cells expressing SLC26A6 and a halide-sensitive

^a Department of Pediatrics, University of California, San Francisco, San Francisco, CA, USA. E-mail: onur.cil@ucsf.edu

^b Department of Medicine, University of California, San Francisco, San Francisco, CA, USA

^c Department of Chemistry and Biochemistry, San Francisco State University, San Francisco, CA, USA

† Electronic supplementary information (ESI) available: Synthesis details and spectroscopy data. See DOI: <https://doi.org/10.1039/d3md00302g>

yellow fluorescent protein.¹¹ A lead candidate from this screen was the isoxazolopyrimidine inhibitor PAT1_{inh}-A0001 with low potency ($\sim 5 \mu\text{M}$ IC₅₀) for PAT1 inhibition.

Here, we optimized isoxazolopyrimidine PAT1 inhibitors by medicinal chemistry and showed the efficacy of a potent inhibitor in blocking intestinal fluid absorption in wildtype and CF mice.

Results and discussion

Structure–activity relationships for isoxazolopyrimidine PAT1 inhibitors

Structure–activity studies of 377 commercially available isoxazolopyrimidine analogues identified 36 active

compounds. The inhibitors contain a core isoxazolo[5,4-*d*]pyrimidine pyrimidine heterocycle with substitutions at the C3 (R^2), C4 (R^3) and C6 (R^1) positions (Fig. 1). In terms of the R^1 moiety, ethyl ester substitution produced the only active SLC26A6 inhibitors whereas a methyl group or a proton abolished activity. To investigate the structural determinants of the SLC26A6 inhibition activity, we evaluated substitution at two positions (R^2 and R^3); since R^1 was found to be optimal as ethyl carboxylate, it was fixed as such in the subsequent studies (Table 1). In terms of the R^2 moiety, a methyl group yielded the most potent inhibitors whereas an ethyl group reduced activity. At R^2 , a 4-fluorophenyl group also maintained moderate inhibitor potency although a phenyl group with alternative substitutions, including 2- and

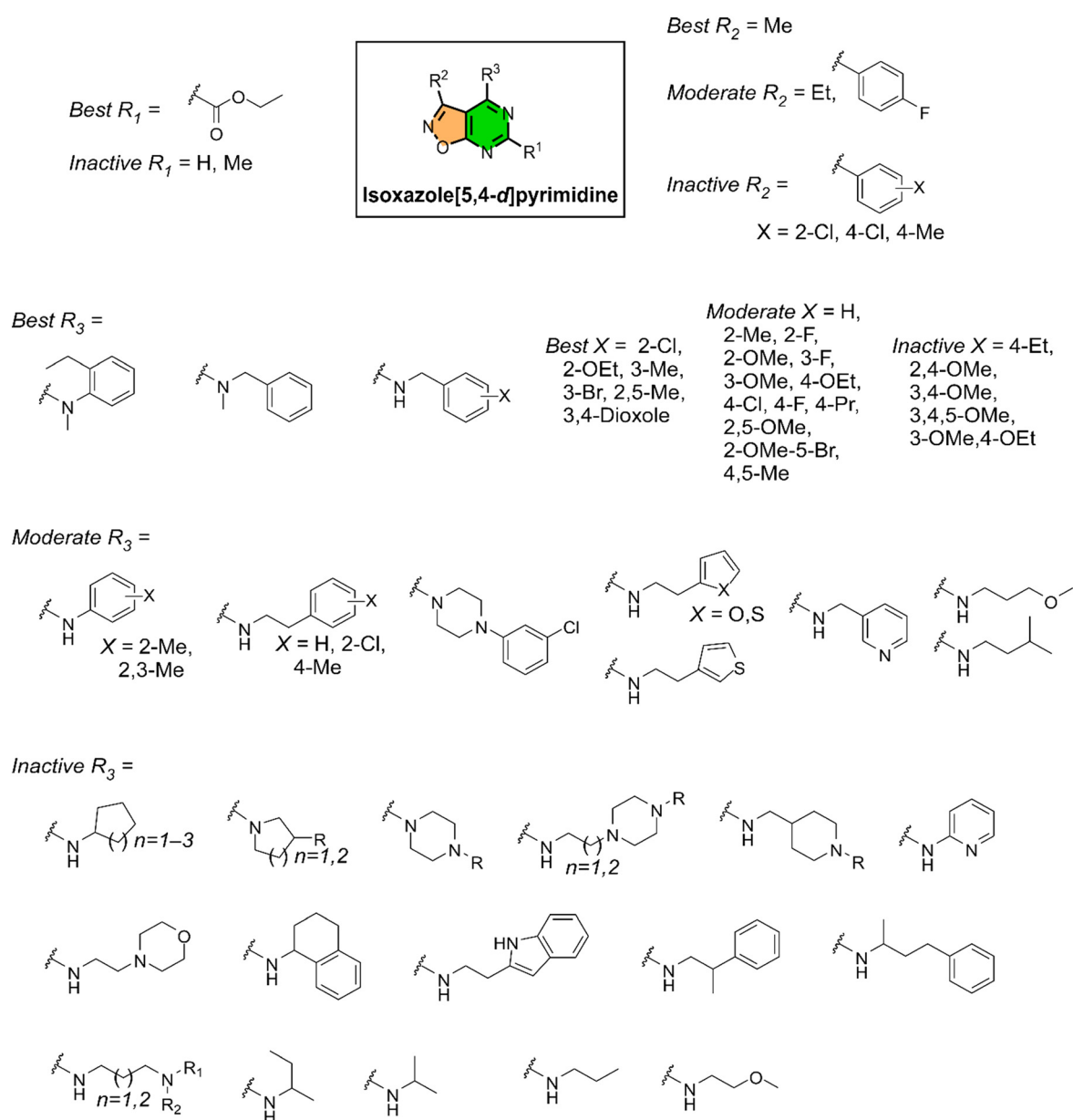


Fig. 1 Summary of SAR data for isoxazolopyrimidine inhibitors of SLC26A6. Best and moderate were used as general terms for classifying different moieties based on potency data, and they refer to the top 1/3 and bottom 2/3 of the active moieties, respectively.

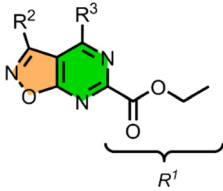
4-chloro or 4-methyl, abolished activity. At the R³ position, the most potent compounds contained a 2-ethyl-*N*-methylaniline or an *N*-methylbenzylamine (A0030) group. A variety of substituted benzylamines at R³ also yielded potent SLC26A6 inhibitors, including compounds with 2-fluoro- (A1286), 2-chloro- (A0207), 2-ethoxy- (A0159), 3-methyl- (A1145) and 3-bromo- (A1339) substitutions on the phenyl moiety. In contrast, distinct substitution on benzylamines at R³ either reduced (*e.g.*, 2-methyl-, 2-methoxy-, 3-fluoro- and 3-methoxy-) or abolished (4-ethyl-, 2,4- or 3,4-methoxy- and 3,4,5-methoxy-) inhibitor activity. Among the benzylamines at R³, it appears that substitution at the 2-, 3-, and 2,3-positions may be best tolerated, while substitution at the 4-position

leads to decreased or abolished activity. Several alternative R³ groups yielded SLC26A6 inhibitors with moderate potency including anilines, phenylethanamines, 2-(thiophen-2-yl)ethanamine, 2-(furan-2-yl)ethanamine, and pyridin-3-ylmethanamine. Finally, more different R³ substitutions abolished SLC26A6 inhibitor activity including amines linked to cyclopentane, cyclohexane, cycloheptane, pyridine, piperazines, piperidines, and indole.

Optimization of isoxazoloimidine PAT1 inhibitors

Using a cell-based assay in FRT cells co-expressing SLC26A6 and a halide-sensitive yellow fluorescent protein (Fig. 2A), the

Table 1 Structure and IC₅₀ of selected class A analogues



Compound (PAT1 _{inh} -XX)	R ²	R ³	IC ₅₀ (μM)
A0030	Methyl	<i>N</i> -Methylbenzylamine	1.0
A1339	Methyl	3-Br-benzylamine	1.1
A1286	Methyl	2-F-benzylamine	1.1
A1145	Methyl	3-Me-benzylamine	1.1
A0207	Methyl	2-Cl-benzylamine	1.1
A0366	Methyl	2,3-Methylphenylamine	1.2
A1528	Ethyl	2-(Furan-2-yl)ethanamine	1.4
A1265	Methyl	2,5-Methylbenzylamine	1.5
A1527	Ethyl	2-(Thiophen-2-yl)ethylamine	1.6
A0270	Methyl	2-(Thiophen-3-yl)ethylamine	1.8
A0292	Methyl	Benzylamine	1.8
A1458	Ethyl	2-OMe-benzylamine	1.9
A1316	Methyl	4-OEt-benzylamine	2.0
A1343	Methyl	3-F-benzylamine	2.2
A0136	Methyl	Isopentylamine	2.3
A0048	Methyl	4-F-benzylamine	2.3
A1340	Methyl	2-Me-benzylamine	2.4
A0319	Methyl	2-(Furan-2-yl)ethanamine	2.4
A1524	Ethyl	2-OMe-5-Br-benzylamine	2.5
A0039	Methyl	1-(3-Chlorophenyl)-4-piperazine	2.6
A1312	Methyl	4-Methylthiobenzylamine	2.6
A1447	Ethyl	Phenethylamine	3.2
A1461	Ethyl	4-F-benzylamine	3.2
A1894	4-F-phenyl	(Pyridin-3-yl)methylamine	3.4
A1396	Ethyl	4-Cl-benzylamine	3.4
A1522	Ethyl	2,5-OMe-benzylamine	3.7
A0194	Methyl	2-Methylphenylamine	3.7
A1448	Ethyl	4-Me-phenethylamine	3.8
A1387	Ethyl	Benzylamine	4.3
A0197	Methyl	3-OMe-benzylamine	4.4
A1991	4-F-phenyl	2-OMe-propanamine	5.1
A1400 (A01)	Ethyl	(4-Chlorophenyl)ethylamine	5.2
A1512	Ethyl	2-F-benzylamine	5.2
A1541	Ethyl	2-Cl-phenethylamine	5.2
A1342	Methyl	4-OPr-benzylamine	5.7
A1341	Methyl	4-Isopropoxybenzylamine	6.5
A0038	Methyl	2-OMe-benzylamine	17.2
A2050	4-F-phenyl	3-Br-benzylamine	Inactive ^a
A0159	Methyl	2-OEt-benzylamine	Inactive ^a

^a <25% inhibition at 25 μM.

original isoxazolopyrimidine inhibitor PAT1_{inh}-A0001 had an IC₅₀ of 5.2 μM for PAT1 inhibition. The most potent compound from SAR studies, PAT1_{inh}-A0030, had a 5-fold improved potency (1.0 μM IC₅₀) compared to PAT1_{inh}-A0001 (Fig. 2B and C).

Synthesis and characterization of PAT1_{inh}-A0030

We developed a synthetic route for isoxazole-containing PAT1 class A inhibitors as the synthesis of this specific class of molecules has not been previously reported (Fig. 3). 5-Amino-3-methylisoxazole-4-carboxylic acid amide (**1**) was treated with ethyl triethoxyacetate (**2**) in the presence of acetic anhydride to generate a cyclic isoxazolopyrimidine derivative (**3**). Treatment of this lactam with phosphorus oxychloride, in the absence of additional solvent, provided a chlorimine derivative (**4**), which was found to be isolable and relatively stable, and did not require purification prior to the subsequent amine substitution reaction. Treatment of **4** with substituted benzylamines and DIPEA provided the final compounds (**5a–5c**) with the various benzylamines linked through an amidine linkage. The crude products were ~95% pure by LCMS; however they were still subjected to chromatography to achieve homogeneous crystalline products, with the absence of detectable impurities by NMR and LCMS, and in good yield of 40–55%.

A literature search on the final inhibitor scaffold (*e.g.*, **5a**, **5b**, and **5c**) showed very little, with only papers useful for the synthesis of related molecules.^{15–17} In terms of reported biological activity, the central scaffold conjugated through amidine linkages to various amines was shown to have anti-malaria activity, by inhibiting *Plasmodium falciparum* dihydroorotate dehydrogenase.¹⁸ Other classes of related molecules were reported as potent tubulin polymerization inhibitors,^{19,20} and inhibitors of kinesin spindle protein with potential anti-cancer activity²¹ or apoptosis-inducing cytotoxic activity.²² The central isoxazolopyrimidine scaffold (with the ester and amidine functionalities removed) has been shown to possess activity against Gram positive and Gram negative

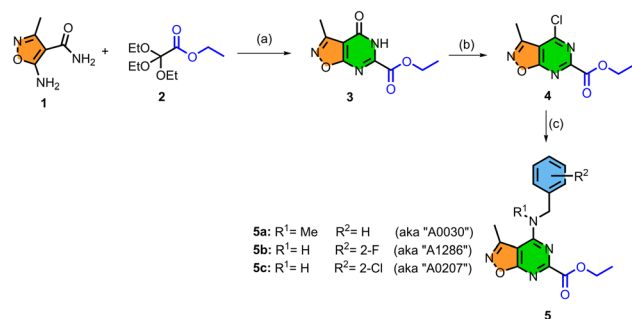


Fig. 3 Synthesis of isoxazole inhibitors of SLC26A6. Reagents and conditions: (a) ethyl triethoxyacetate (**2**, 6 eq.), acetic anhydride (7 eq.); (b) phosphorus oxychloride (30 eq.); (c) substituted benzylamine (1.1 eq.), DIPEA (10 eq.), CH₃CN (0.3 M).

bacteria, and pathogenic fungi.²³ The ethyl ester functionality found in the inhibitor scaffold (*e.g.*, **5a–5c**) may have potential stability issues at low pH or in the presence of esterases. Future studies assessing the activity of the free acid form of the compounds and stability may be informative prior to further preclinical development of these inhibitors.

Selectivity and toxicity of PAT1_{inh}-A0030

To investigate its selectivity, PAT1_{inh}-A0030 was tested for its activity against other members of the SLC26 family and related ion channels. Using FRT cells transfected with halide-sensitive YFP and the respective ion channel/transporter, we found that PAT1_{inh}-A0030 does not inhibit SLC26A3, SLC26A4 or SLC26A9 at a high concentration (Fig. 4A). In similar assays, PAT1_{inh}-A0030 also did not affect the activities of Cl⁻ channels CFTR or TMEM16A (Fig. 4B). PAT1_{inh}-A0030 also did not affect the cell viability after 24 h treatment at high concentration (Fig. 4C).

Efficacy of PAT1_{inh}-A030 in mouse intestinal fluid absorption models

Since PAT1 is prominently expressed in the luminal surface of the ileum, the efficacy of PAT1_{inh}-A0030 was tested in a mouse

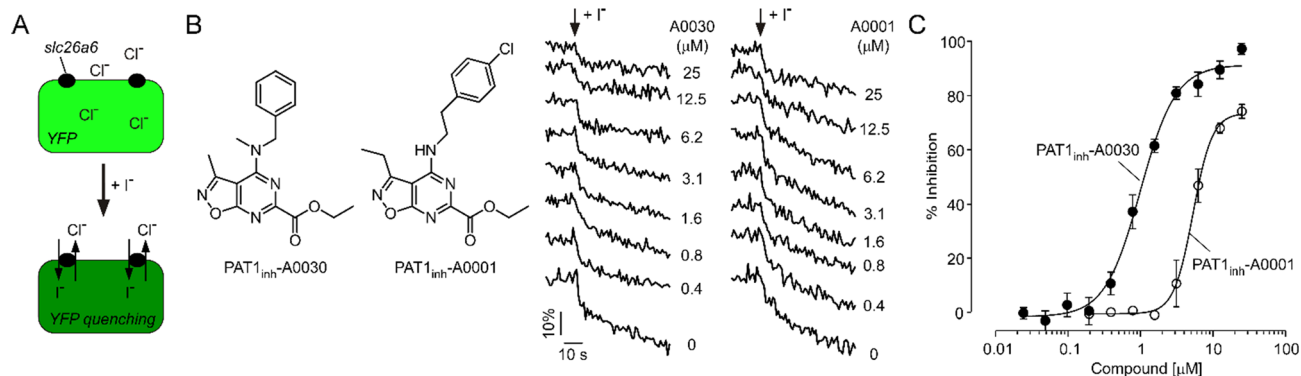


Fig. 2 PAT1 inhibition by the original and improved inhibitors. A. Screening assay in which FRT cells co-expressing slc26a6 (PAT1) and a halide-sensing yellow fluorescent protein (YFP) were subjected to an inwardly directed iodide (I⁻) gradient. PAT1-mediated influx of I⁻ in exchange for Cl⁻ reduces cytoplasmic YFP fluorescence. B. Structures and representative fluorescence traces for PAT1_{inh}-A0030 and PAT1_{inh}-A0001. C. Concentration-response curves of PAT1_{inh}-A0030 and PAT1_{inh}-A0001 for PAT1 inhibition (mean ± S.E.M., *n* = 3–5 per compound per concentration).

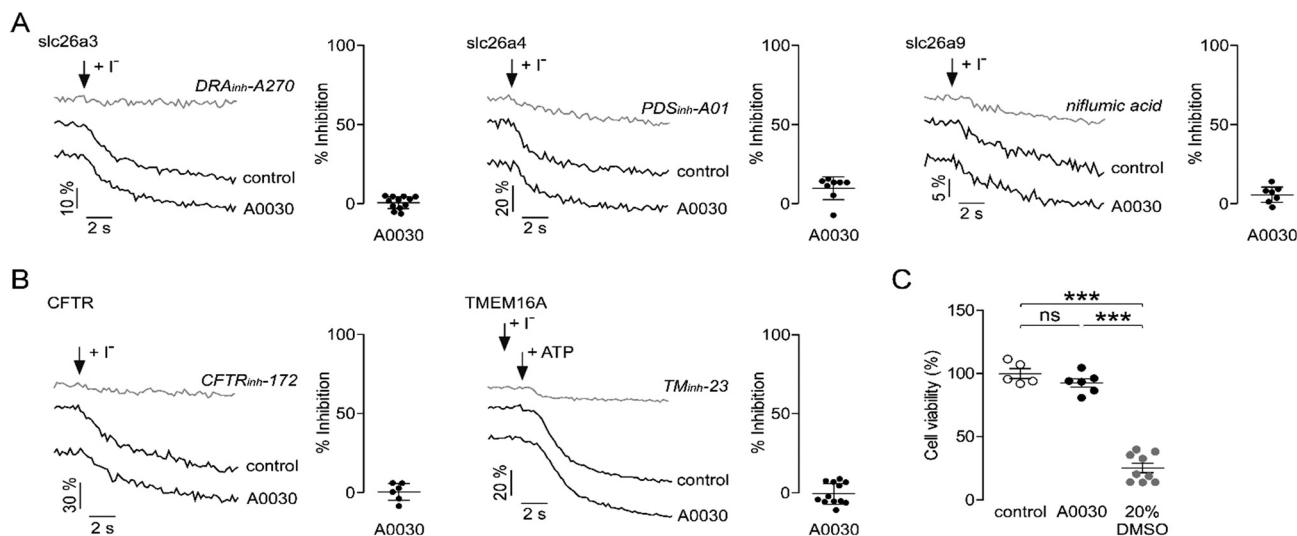


Fig. 4 Selectivity and cytotoxicity of PAT1_{inh}-A0030. Selectivity of PAT1_{inh}-A0030 against related SLC26A family members (A) and Cl⁻/I⁻ channels (B). Cl⁻/I⁻ exchange or I⁻ influx was measured in FRT cells coexpressing YFP and the respective ion transporter/channel, with data shown for 25 μM PAT1_{inh}-A0030, DMSO vehicle control, and positive controls for each transporter/channel (10 μM DRA_{inh}-A270 for SLC26A3, 25 μM PDS_{inh}-C01 for SLC26A4, 500 μM niflumic acid for SLC26A9, 10 μM TM_{inh}-23 for TMEM16A, 10 μM CFTR_{inh}-172 for CFTR). Percentage inhibitions of Cl⁻/I⁻ exchange or I⁻ influx are shown next to the representative fluorescence traces for each transporter/channel. C. Cell viability assayed using Alamar blue in FRT cells incubated for 24 hours with vehicle control (0.1% DMSO) or 10 μM PAT1_{inh}-A0030. 20% DMSO was used as positive control. Mean ± S.E.M., *n* = 5–12 experiments per group, one-way ANOVA and *post hoc* Newman–Keuls multiple comparisons test, ****p* < 0.001, ns: not significant.

intestinal closed-loop model in this segment by intraluminal administration. Animal experiments were performed in accordance with the Guide for the Care and Use of Laboratory Animals by the National Institutes of Health and approved by the UCSF Institutional Animal Care and Use Committee. In this model, the inhibitors are directly injected to the loops, and after 30 minutes, the reduction in loop weight/length ratio and loop fluid volume allows the quantification of intestinal fluid absorption. For these studies, 30 μM PAT1_{inh}-A0030 was used since it fully inhibits PAT1 at this concentration as shown in Fig. 2C. In wildtype mouse ileum, intraluminal PAT1_{inh}-A0030

treatment largely (>90%) prevented the reduction in loop weight/length ratio (Fig. 5A) and loop fluid volume (Fig. 5B), which demonstrates its anti-absorptive effect. Sodium/hydrogen exchanger 3 (NHE3) is the key transporter mediating Na⁺ absorption in the small intestine and is thought to work in tandem with SLC26 anion exchangers for NaCl absorption from the lumen.⁶ As a positive control, we used the NHE3 inhibitor tenapanor in this loop model, which inhibited the reduction in loop weight/length ratio and loop fluid volume to a similar extent as PAT1_{inh}-A0030.

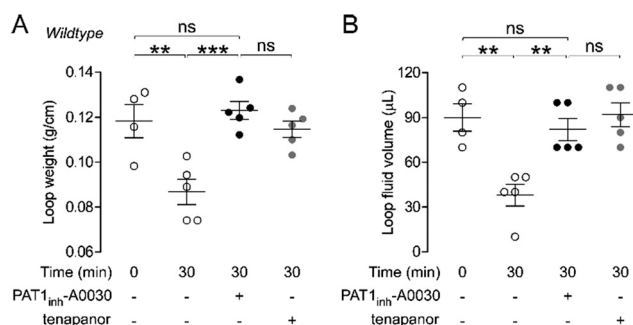


Fig. 5 PAT1_{inh}-A0030 blocks fluid absorption in mouse ileum. Effects of PAT1_{inh}-A0030 (30 μM) and tenapanor (10 μM, NHE3 inhibitor, positive control) on loop weight/length ratio (A) and loop fluid volume (B) in ileal closed loops of wildtype CD1 mice (*n* = 4–5 loops per group). Loops were injected with 100 μL of PBS containing compounds (or 0.1% DMSO control) at zero time and excised at indicated time points for quantification of weight/length ratio and fluid volume. Mean ± S.E.M., one-way ANOVA and *post hoc* Newman–Keuls multiple comparisons test, ***p* < 0.01, ****p* < 0.001, ns: not significant.

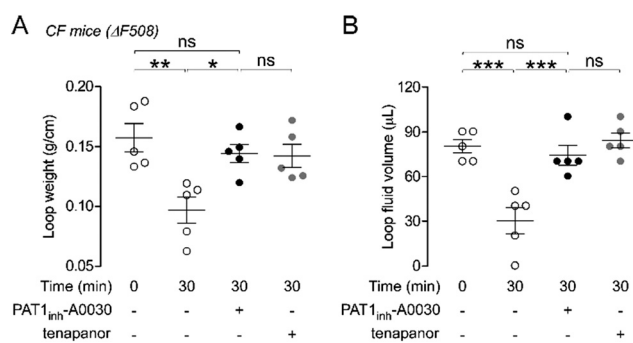


Fig. 6 PAT1_{inh}-A0030 blocks fluid absorption in cystic fibrosis mice. Effects of PAT1_{inh}-A0030 (30 μM) and tenapanor (10 μM, NHE3 inhibitor, positive control) on loop weight/length ratio (A) and loop fluid volume (B) in ileal closed loops of cystic fibrosis mice (Cftr^{delF508/delF508}, *n* = 5 loops per group). Loops were injected with 100 μL of PBS containing compounds (or 0.1% DMSO control) at zero time and excised at indicated time points for quantification of weight/length ratio and fluid volume. Mean ± S.E.M., one-way ANOVA and *post hoc* Newman–Keuls multiple comparisons test, ***p* < 0.01, ****p* < 0.001, ns: not significant.

Since diseases affecting the ileum are common in CF, we used a mouse model of CF harboring the most common CFTR mutation ($Cftr^{delF508/delF508}$) to test the efficacy of PAT1_{inh}-A0030 in a more clinically relevant model. In ileal closed-loops of CF mice, PAT1_{inh}-A0030 inhibited the reduction in loop weight/length ratio and loop fluid volume by >90% (Fig. 6), suggesting the potential efficacy of PAT1 inhibitors in CF-associated GI problems.

Conclusions

Here we optimized isoxazolopyrimidine PAT1 inhibitors and showed that the most potent lead candidate is effective in blocking fluid absorption in the ileum. SAR information was identified which highlights the importance of ethyl ester at R¹, methyl at R², and various substituted benzylamino groups at R³. A concise three step synthesis was developed, providing access to the most potent inhibitors that were identified, in good yield and purity. PAT1 inhibitors can be developed as novel drug candidates for diseases affecting the ileum, particularly meconium ileus and DIOS in CF patients.

Author contributions

TC, PMH, JAT, RM and KR performed the biological experiments and analysed data. JK and MOA performed chemistry and analytical experiments. OC supervised the study, obtained funding and wrote the paper. JK, ASV and MOA revised the paper. The manuscript was reviewed and approved by all authors.

Conflicts of interest

There are no conflicts to declare.

Acknowledgements

This study was supported by grants from the NIH (DK126070, DK072517) and Cystic Fibrosis Foundation.

References

- 1 J. Tobias, M. Tillotson, L. Maloney and E. Fialkowski, *Surg. Clin. North Am.*, 2022, **102**, 873–882.
- 2 T. Kelly and J. Buxbaum, *Dig. Dis. Sci.*, 2015, **60**, 1903–1913.
- 3 B. Moshiree, A. J. Freeman, P. T. Vu, U. Khan, C. Ufret-Vincenty, S. L. Heltshe, C. H. Goss, S. J. Schwarzenberg, S. D. Freedman, D. Borowitz and M. Sathe, *J. Cystic Fibrosis*, 2023, **22**, 266–274.
- 4 C. Colas, P. M.-U. Ung and A. Schlessinger, *MedChemComm*, 2016, **7**, 1069–1081.
- 5 S. L. Alper and A. K. Sharma, *Mol. Aspects Med.*, 2013, **34**, 494–515.
- 6 P. M. Haggie, O. Cil, S. Lee, J.-A. Tan, A. A. Rivera, P.-W. Phuan and A. S. Verkman, *JCI Insight*, 2018, **3**, e121370.
- 7 S. Lee, O. Cil, P. M. Haggie and A. S. Verkman, *J. Med. Chem.*, 2019, **62**, 8330–8337.
- 8 O. Cil, P. M. Haggie, J.-A. T. Tan, A. A. Rivera and A. S. Verkman, *JCI Insight*, 2021, **6**, e147699.
- 9 O. Cil, M. O. Anderson, L. de Souza Goncalves, J.-A. Tan, P. M. Haggie and A. S. Verkman, *Eur. J. Med. Chem.*, 2023, **249**, 115149.
- 10 O. Cil, P. M. Haggie, P.-w. Phuan, J.-A. Tan and A. S. Verkman, *J. Am. Soc. Nephrol.*, 2016, **27**, 3706–3714.
- 11 O. Cil, T. Chu, S. Lee, P. M. Haggie and A. S. Verkman, *JCI Insight*, 2022, **7**, e153359.
- 12 A. Kato and M. F. Romero, *Annu. Rev. Physiol.*, 2011, **73**, 261–281.
- 13 P. Höglund, S. Haila, J. Socha, L. Tomaszewski, U. Saarialho-Kere, M.-L. Karjalainen-Lindsberg, K. Airola, C. Holmberg, A. de la Chapelle and J. Kere, *Nat. Genet.*, 1996, **14**, 316–319.
- 14 R. W. Freel, J. M. Whittamore and M. Hatch, *Am. J. Physiol. Gastrointest. Liver Physiol.*, 2013, **305**, G520–G527.
- 15 S. B. Aliabiev, R. V. Bykova, D. V. Kravchenko and A. V. Ivachtchenko, *Lett. Org. Chem.*, 2007, **4**, 273–280.
- 16 S. B. Alyabiev, D. V. Kravchenko and A. V. Ivachtchenko, *Mendeleev Commun.*, 2008, **18**, 144–146.
- 17 A. Miyashita, K. Fujimoto, T. Okada and T. Higashino, *Heterocycles*, 1996, **2**, 691–699.
- 18 S. Kokkonda, F. El Mazouni, K. L. White, J. White, D. M. Shackelford, M. J. Lafuente-Monasterio, P. Rowland, K. Manjаланagara, J. T. Joseph and A. Garcia-Pérez, *ACS Omega*, 2018, **3**, 9227–9240.
- 19 S. Banerjee, F. Mahmud, S. Deng, L. Ma, M.-K. Yun, S. O. Fakayode, K. E. Arnst, L. Yang, H. Chen and Z. Wu, *J. Med. Chem.*, 2021, **64**, 13072–13095.
- 20 S. Banerjee, K. E. Arnst, Y. Wang, G. Kumar, S. Deng, L. Yang, G.-b. Li, J. Yang, S. W. White and W. Li, *J. Med. Chem.*, 2018, **61**, 1704–1718.
- 21 M.-E. Theoclitou, B. Aquila, M. H. Block, P. J. Brassil, L. Castriotta, E. Code, M. P. Collins, A. M. Davies, T. Deegan and J. Ezhuthachan, *J. Med. Chem.*, 2011, **54**, 6734–6750.
- 22 N. B. Gaikwad, S. Bansod, A. Mara, R. Garise, N. Srinivas, C. Godugu and V. M. Yaddanapudi, *Bioorg. Med. Chem. Lett.*, 2021, **49**, 128294.
- 23 O. Cherif, F. Masmoudi, F. Allouche, F. Chabchoub and M. Trigui, *Heterocycl. Commun.*, 2015, **21**, 191–194.